ASEAN Engineering Journal

Full Paper

SIMULATION OF THE PROPERTIES OF A357 ALUMINUM ALLOY IN SEMI-SOLID STATE FOR EXTRUSION ADDITIVE MANUFACTURING OF METAL

Truong Minh Nhat[a,b,c], Truong Quoc Thanh[a,b], Ngo Ha Quang Thinh[a,b], Tran Trong Quyet[a,b,d], Nguyen Thanh Hai[a,b,*]

[a]Faculty of Mechanical Engineering, Ho Chi Minh City University of Technology (HCMUT), 268 Ly Thuong Kiet, District 10, Ho Chi Minh, Vietnam
[b]Vietnam National University-Ho Chi Minh City (VNU-HCM), Linh Trung Ward, Thu Duc City, Ho Chi Minh, Vietnam
[c]Cao Thang Technical College, 65 Huynh Thuc Khang Street, Ben Nghe Ward, District 1, Ho Chi Minh City
[d]Tran Dai Nghia University (TDNU), 189 Nguyen Oanh Street, Ward 10, Go Vap District, Ho Chi Minh City

Article history
Received
15 June 2024
Received in revised form
02 September 2024
Accepted
11 September 2024
Published online
31 May 2025

*Corresponding author
haint@hcmut.edu.vn

Graphical abstract

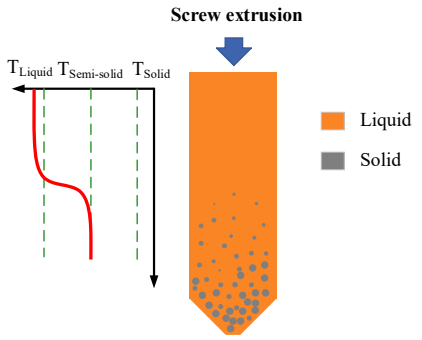

Abstract

In general, the primary issues related to the present design are primarily the high temperature range, which is generating enormous thermal loads to the machinery, and the inability of achieving even temperature distribution in the workpiece. The new approach in this paper mitigates these issues for the aluminum alloy extrusion process using a screw extruder equipped with a Double Wave Screw (DWS). The extrusion screw is typically divided into three regions: the feeding region, the compression region, and the metering region. The DWS component is designed for the compression and metering regions to achieve maximum shear rate in extrusion, to create globular microstructure. Furthermore, our work aims to predict significant process parameters such as viscosity, shear rate, and material flow velocity to determine the feasibility of 3D printing. In order to validate the effectiveness of the material extrusion process in the 3D printing process, the model has been simulated through the finite element method (FEM) by employing the power-law model, which describes the non-Newtonian behavior of the composite semi-liquid aluminum needle. Simulation has demonstrated that control of the material outlet temperature can generate a semi-liquid state of aluminum. Besides, the DWS configuration enhances the shear rate and homogeneity of the molten metal, ultimately leading to enhanced mechanical properties of the product extruded.

Keywords: Extrusion screw, semi-solid, globular microstructure, additive manufacturing, Non-Newtonian fluid, laminar flow.

1.0 INTRODUCTION

Extrusion is a very ubiquitous process to produce materials utilized in industries such as plastics, polymers, and the pharmaceutical industry [1]. Most of the materials of these processes need the non-Newtonian state [2-4], in which their flow behavior is dependent on the shear rate. The nature of this state is quite different compared to the behavior of water and air, which are Newtonian fluids. Additive manufacturing, more commonly referred to as 3D printing, has made enormous strides in recent years. It is a technique that can usher in a new revolution in different industries by designing metal parts of complex geometries with improved properties [5-7]. Amongst metal 3D printing techniques, screw extrusion has evolved as an appropriate process for producing metal parts [8-10].

One metal that has attracted significant attention in screw extrusion-based metal 3D printing is aluminum (Al). Aluminum boasts excellent properties, including low density, high strength-to-weight ratio and excellent thermal and electrical

conductivity, making it an attractive material for a variety of applications. However, due to the easily oxidized nature of aluminum, the effective application of this material in screw extruded metal 3D printing poses some challenges [11, 12]. Oxidation limits the bond between printed material layers. Despite these challenges, aluminum is still a promising material for application in the field of metal 3D printing. Good control of process parameters can help solve these challenges. From there, create high-quality parts from metal 3D printing.

Additive manufacturing (AM) is a rapidly growing technology field, with the potential to revolutionize manufacturing processes. This is a complex and challenging field, involving many factors to consider such as materials, equipment design and process parameters. One aspect of interest is to understand the rheological behaviors, such as shear rate, viscosity and shear stress of semi-fluid materials, especially ADC12 aluminum alloy [13]. Additionally, the Polyflow simulation platform has been used to model and analyze plastic injection molding processes involving non-Newtonian materials with single-screw extruders [14]. There are also innovative approaches in the realm of 3D printing for semi-liquid metals. For instance, researchers have adapted a Filabot EX2 polymer fiber extruder into a mixing and extrusion device to work with thixotropic alloys [15]. In a similar vein, investigators in [16] explored 3D printing of CuSn10 bronze using a screw-driven extrusion method, aiming to reduce costs compared to other 3D printing techniques. Their research highlighted the significant influence of printing process parameters on the properties of printed components. However, much of the existing research primarily focuses on plastics, polymers, or low-melting materials, with limited attention given to materials with high-temperature domains such as metals. Therefore, this study has a specific focus on simulating the properties of aluminum alloy during extrusion and developing metal 3D printing equipment based on the extrusion method. This endeavor lays the groundwork for further research and development in the field of metal 3D printing via extrusion methods.

The heat treatment process is also carefully studied, as it is an important factor in achieving the desired material state, Table 1. Two alloys, Sn-15Pb and Pb-40Sn, were chosen to study the Semi-Solid Metal Extrusion Device (SSMED) process. The choice of these alloys is due to the low processing temperature and large semi-solid phase region, which are well suited to the capabilities of the SSMED device [17]. Furthermore, semi-solid extrusion equipment is specifically designed to operate effectively under harsh conditions such as high temperatures. Therefore, extrusion equipment has become the focus of recent interest and research. For plunger-based 3D printing devices, this configuration poses challenges in controlling outlet pressure due to volume and temperature variations [18]. Besides, Filament-based configuration is applied to Mg-Zn alloys, which are biodegradable. This shows great potential in applying 3D thixo-printing technology to the medical field. This research provides a solution to avoid the need for re-surgery, the support structure will naturally decompose in the body. Thereby limiting the existence of harmful debris from medical equipment when inserted into the body as before [19]. The researchers also designed and manufactured a single screw extruder, with a screw diameter of 8 mm, used to extrude materials ethylene vinyl acetate and poly 1-vinylpyrrolidon-co-vinyl acetate. This device helps 3D printing directly from powder form [20]. Additionally, the design and fabrication of Fused Deposition Modeling (FDM) equipment utilizing a suitable screw extruder system to handle high-load solid materials have been explored. To achieve a stable output speed and material mass, various parameters, including cylinder temperature, nozzle diameter, and screw speed, have been calculated and optimized within this research context [21].

However, the majority of research in this field has primarily concentrated on plastics, polymers, or materials with low melting points. Materials with high-temperature characteristics, such as metals, have not received as much attention. Consequently, this study is specifically directed toward simulating the properties of aluminum alloy during the extrusion process and the development of metal 3D printing equipment based on the extrusion method. This endeavor lays the foundation for further research and development of metal 3D printing techniques employing extrusion. One notable advantage of using semi-solid metal with high viscosity lies in its ability to prevent macroscopic turbulence during die-filling, thereby reducing potential part defects resulting from air entrapment [22]. Another advantage stems from the high solid fraction, approximately 40%, in the 3D printing process, which minimizes volume loss during complete solidification, consequently mitigating shrinkage porosity or permitting greater cross-sectional changes than other 3D printing methods allow. This method capitalizes on both liquid and solid formation processes. In the absence of shear force, the semi-solid slug exhibits solid-like characteristics, such as the ability to maintain its shape, while the application of shear significantly reduces viscosity, allowing the material to flow like a fluid, i.e., it adopts a thixotropic state [23]. Furthermore, the lower process temperature associated with semi-solid metal can lead to a substantial increase in tool lifespan compared to other 3D printing methods, particularly those using metals in a liquid state. Hence, this study centers on simulating the properties of aluminum alloy during the extrusion process and the development of metal 3D printing equipment utilizing the extrusion method, laying the foundation for further exploration and research into metal 3D printing methods based on extrusion.

In this study, the model uses ADC12 aluminum alloy material for simulation, which is extruded through a nozzle with a screw with an outer diameter of 30 mm and a variable depth of the channels. The finite element method is used on COMSOL software for simulation to determine the properties of aluminum when extruded in a semi-liquid state such as temperature distribution, viscosity, shear rate, and velocity.

Table 1 Summary of some researches on metal 3D printing using screw extrusion method

Category	Author(s)	Publication year	Specification	Advantage(s)	Limitation(s)
Semi-solid state	Amin Jabbari et al [17]	2018	A new method for additive manufacturing of metals in semi-solid state using thixo-extrusion.	More sustainable, can fabricate complex geometries, more cost-effective.	Thixotropic properties, defects, efficiency and cost.
3D thixo-printing	Dalton Daniel Lima et al [19]	2020	Uses a fused filament fabrication (FFF) technique to print biodegradable Mg-Zn alloys in the semi-solid state.	Simple, cost-effective, can fabricate complex geometries with high accuracy and surface finish, environmentally friendly.	Still under development, challenges with controlling the semi-solid state and preventing defects, not as widely used as other additive manufacturing techniques.
Screw extrusion	Ahmet Çağrı Kılınç et al [16]	2021	Developed a 3D printer extrusion for molten CuSn10 alloy, investigated the printing parameters.	Simple ad cost effective, can fabricate complex geometries, good mechanical properties.	Ensitive to printing parameters, may have defects, not yet widely used.
Screw extrusion, FDM	Tim Feuerbach and Markus Thommes [20]	2021	Design and characterization of a screw extrusion hot-end for FDM.	Can print a wider range of materials, more efficient, more consistent.	More complex and expensive, may not be suitable for all materials.
Screw extrusion, FDM	Qinglong He et al [21]	2021	Fused deposition modeling (FDM) with screw extrusion.	Can be used to fabricate dense zirconia ceramics with high accuracy and repeatability.	Processing window is narrow.
Metal 3D printing, thixotropic materials	Yifan Fei et al [15]	2022	New method for direct thixotropic metal 3D printing, fabricate thixotropic alloys.	Cost-effective and efficient than current powder-based metal 3D printing methods, thixotropic materials are easier to process than powder materials, create complex geometries.	The thixotropic properties of alloys can be sensitive to changes in temperature and shear rate.

2.0 METHODOLOGY

2.1 Geometric model

In this research, the screw is an important component, consisting of three separate parts, each responsible for a specific function. The first section, called the feeding section or Zone A in Figure 1a, plays a key role in material feeding. It is responsible for putting raw materials into the initial extruder and transporting them. This section is often equipped with a hopper or other feeding device assembly to ensure a continuous supply of material for the extrusion process [21, 24].

The second section (zone B) has a tapered shape, designed so for the purpose of compression and degassing as shown in Figure 1b. Its main function is to facilitate the removal of air or air bubbles trapped inside the material being extruded. This zone plays an important role in achieving uniformity and eliminating voids in the final product. By creating pressure and compressing the material flow, a denser structure is created. This helps improve the properties of the extruded material. The cone angle depends on the compression ratio [25, 26], which is calculated as follows:

$$C = \frac{H_f}{H_m} = \frac{k_T}{k_s} \quad (1)$$

where C – the compression ratio, H_f – the channel depth of the feeding-zone, H_m – the depth of the metering channel, k_T – the isothermal compressibility and k_s – the isentropic or adiabatic compressibility of a liquid.

For aluminum material [26], k_T = 0.0263GPa^{-1} and k_s = 0.0191GPa^{-1}.

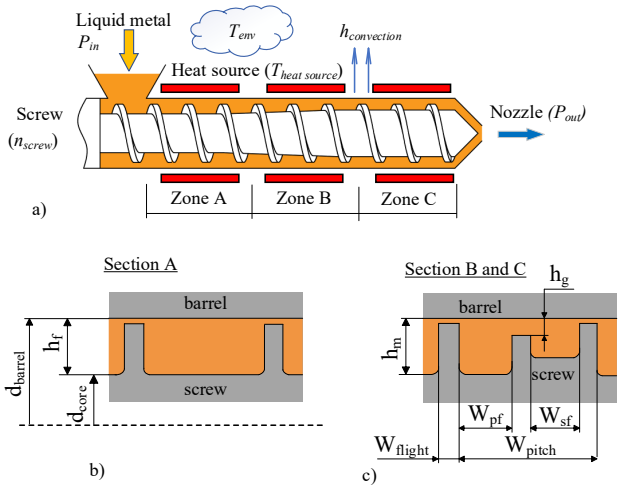

Figure 1. a – Description of the extrusion screw model; b – At the feeding zone; c – At the compression and the metering zone.

The third part (Zone C) is dedicated to stabilizing the molten metal during extrusion. This zone helps maintain a consistent flow and prevents any fluctuations in the material's viscosity. It is essential for achieving precise and consistent extrusion outcomes, ensuring that the final product adheres to the desired specifications [25]. The Double Wave Screw is designed for Zones B and C, as shown in Figure 1c. Its primary purpose is an innovative extruder component designed to enhance the shear rate within the extrusion process [27, 28]. This enhancement helps create a globular microstructure, improving optimal flow, high homogeneity, and mechanical strength [29-32].

The parameters of this physical model and some boundary conditions that were used in the simulation, are presented in Table 2. Assuming that the inner material is considered as an object to simulate. Cylinder with diameter inner 30 mm, length 300mm, outlet diameter 5mm. The rotational speed of the shaft is n_{screw} rpm. Inlet pressure (P_{in}) and outlet pressure (P_{out} = 0). Aluminum A357 is melted at T_{in} = 650 ^{0}C and attached to the tank. Along the extrusion device, there is a heating resistor with a temperature range of $T_{heat\ source}$ = 400 ^{0}C, a convection heat transfer coefficient h =5 W/m^2.K [33] and T_{env} ^{0}C is the ambient temperature, to ensure that the outlet temperature of the material reaches the semi-solid state.

Table 2. List of screw structure parameters.

Symbol	Description	Value
d_{barrel}	Inner diameter of the barrel	30 mm
d_{screw}	Core diameter of extruder screw	20 mm
d_{nozzle}	Diameter of nozzle	5 mm
W_{flight}	Flight width	5 mm
W_{pitch}	Pitch of the extruder screw	20 mm
W_{sf}	Width of secondary flight	8 mm
W_{pf}	Width of primary flight	8 mm
h_f	Depth of the feed channels (Zone A)	5 mm
h_m	Depth of the metering channels (Zone C)	4 mm
h_g	The gap	1.5 mm
L	Total extrusion screw length	300 mm
N_{flight}	Number of parallet flights	1

2.2 Theoretical Assumptions

Assumption 1: Fundamental analysis of thermal mechanical

The heat field in the computational domain is solved using the heat conduction equation combined with the corresponding boundary conditions. This process allows determining the temperature distribution in three-dimensional space of the computational domain based on input factors.

$$\nabla\left(k\nabla T\right)+Q=\rho C_p\frac{\partial T}{\partial t} \quad (2)$$

where k – thermal conductivity depends on temperature, T – temperature field, Q – rate of heat generation per unit volume caused by the laser exposure, P – mass density depends on temperature and C_p – constant-pressure specific heat capacity.

The external surface of the device that is subject to convection and heat radiation is also considered since the device is in direct contact with the atmosphere. The device is placed in a single-phase environment and has no forced convection so choose the convective heat transfer coefficient h = 2 W/m^2.K [33]. The amount of heat released by convection is described based on Newton's law of cooling as follows. [33]

$$q_{conv}=h\left(T_s-T_{env}\right) \quad (3)$$

where h – the convective heat transfer coefficient, T_s – the temperature on the top surface and T_{env} – the temperature of the environment.

The heat loss due to thermal radiation q_{rad} is described according to the Stefan-Boltzmann law: [33]

$$q_{rad}=\varepsilon\sigma\left(T_s^4-T_{env}^4\right) \quad (4)$$

where ε – the surface emissivity and σ – the Stefan-Boltzmann constant.

Assumption 2: Non-Newtonian fluid

A non-Newtonian fluid has special flow properties that differ from a Newtonian fluid. When the graph representing shear stress versus shear rate of this fluid is not a straight line passing through the origin, it means that the apparent viscosity (shear stress versus shear rate) does not maintain a constant value under these conditions. certain temperature and pressure. Instead, apparently the applicable viscosity depends on the flow conditions such as flow geometry, shear rate, and even literature to model shear-thinning characteristics are considered. Aluminum belongs to the domain of shear-thinning [13].

To model the viscosity reduction characteristics according to shear rate of this type of fluid, many mathematical models have been proposed. These mathematical expressions are intended to more accurately simulate and predict the flow behavior of non-Newtonian fluids.

Assumption 3: The power-law or Ostwald de Waele model

Characteristics of shear thinning, the fluid flow curve (Figure 2) can be determined through the ratio between shear rate and shear stress. [23, 34]

$$\tau = m\left(\dot{\gamma}\right)^{n} \tag{5}$$

Therefore, the apparent viscosity of a liquid known as the power law (or Ostwald de Waele) is given by:

$$\mu = \frac{\tau}{\dot{\gamma}} = m\left(\dot{\gamma}\right)^{n-1} \tag{6}$$

where τ – shear stress, m – consistency factor, n – flow behavior index, $\dot{\gamma}$ – shear rate and μ – viscosity.

For μ<1 is the fluid exhibits shear thinning,
μ =1 is the fluid exhibits Newtonian behavior,
μ >1 is the fluid exhibits shear thickening.

The power law model represents the characteristics of fluid flow, gradually diluting with shear rate, but it still has some limitations. This model only applies within a limited shear rate range. This means that the constants m and n in the Power Law equation will be different depending on the shear rate range that is considered. Furthermore, the model fails to predict zero and infinite viscosities.

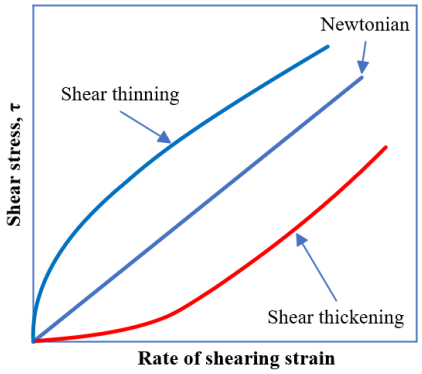

Figure 2 Variation of shearing stress with rate of shearing strain of the fluids. [35]

The equipment in this study is used to extrusion aluminum in a semi-solid state. Therefore, the rheological parameters of the fluid are only considered in the temperature range where A357 aluminum reaches the semi-solid state. In Figure 3, the heating devices are also thermally controlled so that the fluid in the extrusion screw must be maintained at a temperature between 556 °C and 610 °C [36].

In the temperature range 556 °C - 610 °C, parameters fluid consistency coefficient and flow behavior index are presented in Eq. (6) and Eq. (6) [2]. The rheological parameters of the material are shown in Table 3.

$$\log m = -0.094T + 60.263 \tag{7}$$

$$n = \frac{0.44}{1+10^{0.2(T-577)}} + \frac{0.3}{1+10^{0.18(587-T)}} - 0.4 \tag{8}$$

Table 3 Properties of aluminum A357.

Thermal Conductivity [W/(m.K)]	Density [kg/m³]	Heat Capacity [J/(kg.K)]
0.242	2700	2000

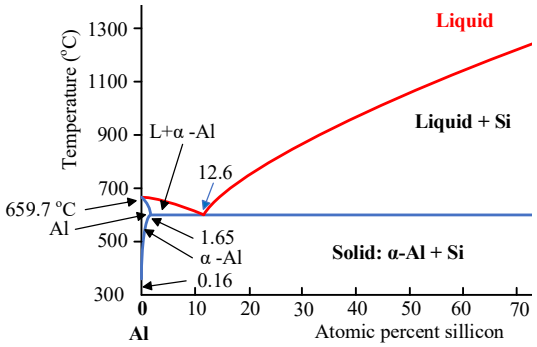

Figure 3 Description of phase diagram for Al-Si cast alloy. [37]

Assumption 4: Creeping flow

Navier-Stockes (N-S) Equations Fluid Dynamics

$$\rho\left(\frac{\partial u}{\partial t} + u\nabla u - f\right) = -\nabla p + \mu\nabla^2 u \tag{9}$$

where ρ – the density of the liquid, t – the time, μ – the kinematic viscosity, u – the velocity vector of the fluid, f – the vector containing the body forces acting on the liquid, p – the fluid pressure, ∇ – the gradient operator and ∇^2 – Laplace operator.

Due to the high viscosity of the material, the Reynolds number, which characterizes the ratio of inertia to viscous forces, is low. At low Reynolds numbers, viscous forces take precedence over inertial forces [38]. Consequently, the latter can be disregarded in the Navier-Stokes equations, and the Creeping Flow interface can be applied. The Creeping Flow Interface models the Navier-Stokes equations without considering the inertia term. This is commonly known as Stokes flow and is suitable for situations with low Reynolds numbers, such as those found in very small channels or microfluidic applications. This physics interface can also handle non-Newtonian fluids, utilizing the Power Law and Carreau models, but it does not account for turbulence [39].

3.0 RESULTS AND DISCUSSION

3.1 Temperature of material flow

Based on the aforementioned boundary conditions, the temperature simulation results are depicted in Figure 4. Along the entire length of the tube, there is a heating element maintaining the tube at a source temperature of 400 °C. This is essential to prevent the aluminum material from solidifying inside the screw, ensuring it remains in a semi-solid state for metal 3D printing. The initial temperature corresponding to molten aluminum is 650 °C, gradually decreasing along the

length of the screw. The resulting temperature at the faucet exit is approximately 550 °C. The decrease in output temperature can be attributed to the temperature difference (relative to the 400 °C heater) and the convection heat transfer coefficient (h= 5 W/m².K). This temperature aligns with the semi-liquid temperature of A357.

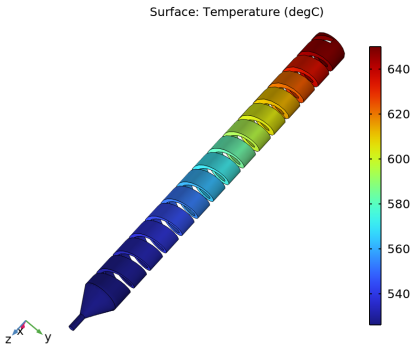

Figure 4. Simulation result of temperature analysis for material flow.

3.2 Velocity Of Material Flow

The velocity simulation results serve to guide device design and predict the conditions for future metal 3D printing processes. According to the simulation results, the material's output velocity is contingent upon the rotational speed of the screw and the input pressure pin. As evident, when in contact with the barrel, the material exhibits a nearly adhesive quality, in line with the theory of non-Newtonian fluid behavior. In this scenario, the fluid's velocity is low when in proximity to a stationary surface (cylinder) and increases when near a moving surface [23, 40]. Initially, the material flow exhibits a relatively slow velocity as shown in Figure 5a and Figure 5b, approximately 100-300x10^{-5} m/s, contingent upon the radial position. The average speed at the Z = 50 mm location is 25x10^{-4} m/s. Subsequently, the material flow velocity that illustrated in Figure 5c and Figure 5d, increases at the Z = 50 mm and Z = 250 mm positions, as it enters the double wave screw zone. This escalation is due to the reduced cross-sectional area at this point, resulting in higher material speeds, with an average velocity of about 30x10^{-4} m/s. At the nozzle position, the aluminum velocity is somewhat reduced as Figure 5e.

3.3 Shear Rate Of Material Flow

In this approach, Zone B and C are designed as Double Wave Screws. The rationale behind this design is to increase shear stress because I. Boumehdi's research [41] demonstrated that it was not possible to achieve a globular microstructure using other configurations. Failure to obtain a globular microstructure can potentially lead to a reduction in the material's mechanical properties [32, 42]. The shear rate simulation results include a comparison between the shear rates of a single screw and a double wave screw, as shown in Figure 7. To obtain these results, a straight line was traced along the screw axis connecting two points: Point 1 (X = 0, Y = 0.014, Z = 0) and Point 2 (X = 0, Y = 0.014, Z = -0.34), with the unit of measurement in meters. Initially, the shear rates for these two types of screws are approximately the same due to the similarity in the structure of this zone. However, in Zone B and C, the shear rate of the double wave screw surpasses that of the single screw, as illustrated in Figure 6 and Figure 7. This enhancement contributes to the transformation of dendritic microstructures into globular ones [31, 43]. Furthermore, these shear rate simulation results align with findings from Zhen Ma's research [2].

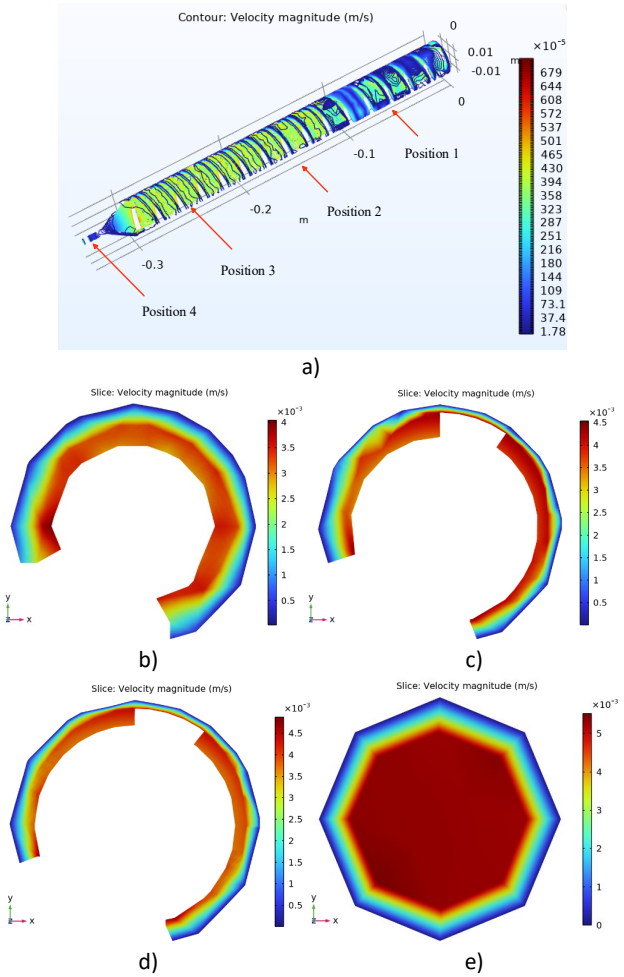

Figure 5. a – Simulation result of the velocity analysis for the material flow; b – Velocity at position 1 (Z = 50mm); c – Velocity at position 2 (Z = 150mm); d – Velocity at position 3 (Z = 250mm); e – Viscosity at nozzle.

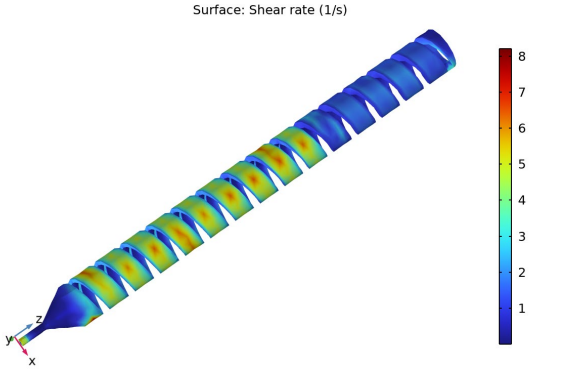

Figure 6 Simulation result of shear rate analysis for the material flow.

3.4 Viscosity Of Material Flow

The viscosity of the aluminum semi-solid was measured at various positions along the length of the screw. The results in Figure 8 show that the viscosity tends to increase gradually from position Z = 50 mm to Z = 250 mm. The primary factor driving this increase is the decrease in temperature along the length of the screw. Additionally, the shear rate also increases as one progresses along the screw length, further contributing to the rise in viscosity [2, 44]. This simulation result shows that the viscosity is suitable for 3D printing with aluminum alloy [45].

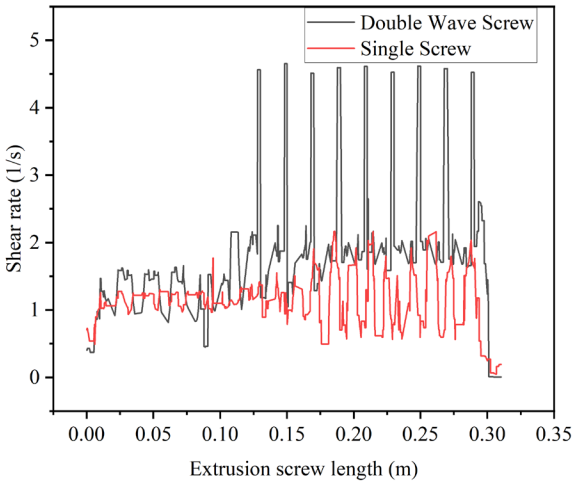

Figure 7 Compare shear rate along screw length between double wave screw and single screw.

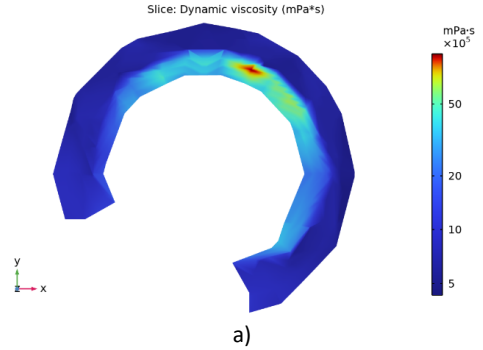

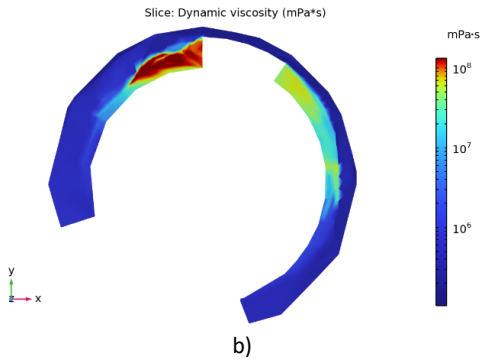

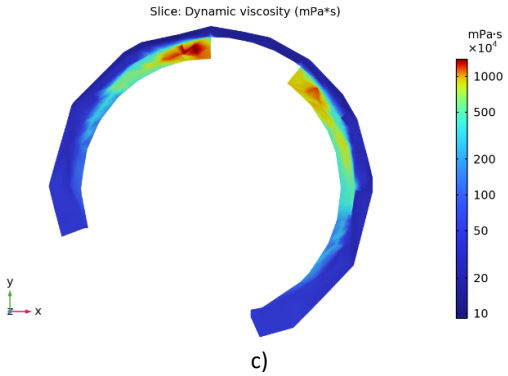

Figure 8 Simulation results of the viscosity analysis for the material flow; a - Viscosity at position Z = 50mm; b - Viscosity at position Z = 150mm; c - Viscosity at position Z = 250mm.

4.0 CONCLUSION AND FUTURE WORK

The results of this research showcase the potential of the screw extruder with the double wave screw for extruding aluminum alloy in a semi-solid state. The Double Wave Screw effectively enhances the flow rate, homogeneity, and mechanical properties of the extruded product. With the input parameters mentioned above, the simulation results lead to the following conclusions: (1) Temperature decreases along the screw length, and with a heating temperature of approximately 400 °C, it is suitable for creating semi-solid materials, ensuring the correct outlet temperature for metal 3D printing. (2) The double wave screw aids in improving the shear rate, increase shear rate from 2 s^{-1} to 5 s^{-1} corresponds to an increase in viscosity from $50x10^2$ Pa.s to 10^4 Pa.s, which facilitates the development of a globular microstructure. (3) The simulation results align with the theoretical foundations established in previous studies. Decreasing temperature causes an increase in viscosity, while increasing shear rate increases viscosity.

In the future work, we will proceed to fabricate, assemble and evaluate the actual device. The actual results will be compared with the simulation results. From there, proceed to improve and adjust the design to the most optimal level.

Acknowledgement

We acknowledge Ho Chi Minh City University of Technology (HCMUT), VNU-HCM for supporting this study.

Conflicts of Interest

The author(s) declare(s) that there is no conflict of interest regarding the publication of this paper

References

[1] S. Singh, S. Ramakrishna, and R. Singh, 2017. "Material issues in additive manufacturing: A review," *Journal of Manufacturing Processes,* 25: 185-200. DOI: https://doi.org/10.1016/j.jmapro.2016.11.006.

[2] Z. Ma, H. Zhang, W. Song, X. Wu, L. Jia, and H. Zhang, 2020. "Pressure-driven mold filling model of aluminum alloy melt/semi-solid slurry based on rheological behavior," *Journal of Materials Science & Technology,* 39: 14-21, 2020/02/15/ DOI: https://doi.org/10.1016/j.jmst.2019.07.048.

[3] Z. Ke, H. Zhongqi, Y. Shupan, and C. J. P. E. Wanghua, "Numerical simulation for exploring the effect of viscosity on single-screw extrusion process of propellant," *Procedia Engineering.* 84: 933-939, 2014. DOI:https://doi.org/10.1016/j.proeng.2014.10.518.

[4] M. V. Karwe and Y. Jaluria, 1990. "numerical simulation of fluid flow and heat transfer in a single-screw extruder for non-newtonian fluids," *Numerical Heat Transfer, Part A: Applications,* 17(2): 167-190. 1990/03/01 DOI: https://doi.org/10.1080/10407789008944738.

[5] K. Wang, C.-C. Ho, C. Zhang, and B. Wang, 2017. "A Review on the 3D Printing of Functional Structures for Medical Phantoms and Regenerated Tissue and Organ Applications," *Engineering,* 3(5): 653-662, 2017/10/01/ DOI: https://doi.org/10.1016/J.ENG.2017.05.013.

[6] J. Jiang, 2020. "A novel fabrication strategy for additive manufacturing processes," *Journal of Cleaner Production,* 272: 122916. 2020/11/01/ DOI: https://doi.org/10.1016/j.jclepro.2020.122916.

[7] J. Gonzalez-Gutierrez, S. Cano, S. Schuschnigg, C. Kukla, J. Sapkota, and C. Holzer, 2018. "Additive Manufacturing of Metallic and Ceramic Components by the Material Extrusion of Highly-Filled Polymers: A Review and Future Perspectives," *Materials.* 11(5): 840. DOI: https://doi.org/10.3390/ma11050840.

[8] N. A. S. Mohd Pu'ad, R. H. Abdul Haq, H. Mohd Noh, H. Z. Abdullah, M. I. Idris, and T. C. Lee, 2020. "Review on the fabrication of fused deposition modelling (FDM) composite filament for biomedical applications," *Materials Today: Proceedings.* 29: 228-232, 2020/01/01/ DOI: https://doi.org/10.1016/j.matpr.2020.05.535.

[9] T. M. Nhat, N. H. Q. Thinh, N. Q. Van, L. Van Nhan, and N. T. Hai, 2024."Analysis of Heat Distribution and Velocity of Shielding Gas Flow in Chamber for Aluminium 3D Printing," in *Conference on Microactuators and Micromechanisms*, 429-441: Springer.

[10] R. V. Pazhamannil, P. Govindan, and P. Sooraj, 2021. "Prediction of the tensile strength of polylactic acid fused deposition models using artificial neural network technique," *Materials Today: Proceedings.* 46: 9187-9193, 2021/01/01/ DOI: https://doi.org/10.1016/j.matpr.2020.01.199.

[11] G. Mathers, 2002. "2 - Welding metallurgy," in *The Welding of Aluminium and its Alloys*, G. Mathers, Ed.: Woodhead Publishing. 10-34.

[12] T. M. Nhat, T. T. Quyet, L. D. Binh, and H. Q. T. Ngo, 2023, "Metal Additive Manufacturing Through Screw Extrusion: State-of-the-Art and Future Prospects," in *EAI International Conference on Renewable Energy and Sustainable Manufacturing*. 343-358: Springer.

[13] A. Kumbhare, P. Biswas, A. Bisen, and C. Choudhary, 2023."Investigation of Effect of the Rheological Parameters on the Flow Behavior of ADC12 Al Alloy in Rheo-Pressure Die-casting," *International Journal of Metalcasting,* 2023/01/31 DOI: https://doi.org/10.1007/s40962-023-00962-6.

[14] Z. Ke, H. Zhongqi, Y. Shupan, and C. Wanghua, 2014. "Numerical Simulation for Exploring the Effect of Viscosity on Single-screw Extrusion Process of Propellant," *Procedia Engineering,* 84: 933-939. 2014/01/01/ DOI: https://doi.org/10.1016/j.proeng.2014.10.518.

[15] Y. Fei, J. Xu, D. Yao, R. Chiou, and J. Zhou, 2022. "Design, simulation, and experiments for direct thixotropic metal 3D printing," *Materials Science in Additive Manufacturing* 1(1), DOI: https://doi.org/10.18063/msam.v1i1.5.

[16] A. Ç. Kılınç, A. A. Goktas, Ö. Y. Keskin, and S. Köktaş, 2021. "Extrusion-Based 3D Printing of CuSn10 Bronze Parts: Production and Characterization," 11(11): 1774,

[17] A. Jabbari and K. Abrinia, 2018. "Developing thixo-extrusion process for additive manufacturing of metals in semi-solid state," *Journal of Manufacturing Processes,* 35: 664-671, 2018/10/01/ DOI: https://doi.org/10.1016/j.jmapro.2018.08.031.

[18] L. Ren *et al.*, 2017 "Process Parameter Optimization of Extrusion-Based 3D Metal Printing Utilizing PW-LDPE-SA Binder System," (in eng), *Materials (Basel),* 10(3): 305. 16. DOI: https://doi.org/10.3390/ma10030305.

[19] D. D. Lima, K. N. Campo, S. T. Button, and R. Caram, 2020."3D thixo-printing: A novel approach for additive manufacturing of biodegradable Mg-Zn alloys," *Materials & Design,* 196: 109161, 2020/11/01/ DOI: https://doi.org/10.1016/j.matdes.2020.109161.

[20] T. Feuerbach and M. Thommes, 2021. "Design and Characterization of a Screw Extrusion Hot-End for Fused Deposition Modeling," *Molecules.* 26: 590, 01/23 DOI: https://doi.org/10.3390/molecules26030590.

[21] Q. He *et al.*, 2021. "Additive manufacturing of dense zirconia ceramics by fused deposition modeling via screw extrusion," *Journal of the European Ceramic Society,* 41(1): 1033-1040, 2021/01/01/ DOI: https://doi.org/10.1016/j.jeurceramsoc.2020.09.018.

[22] B. Wu *et al.*, 2018. "A review of the wire arc additive manufacturing of metals: properties, defects and quality improvement," *Journal of Manufacturing Processes,* 35: 127-139, 2018/10/01/ DOI: https://doi.org/10.1016/j.jmapro.2018.08.001.

[23] R. P. Chhabra and J. F. Richardson, 1999,"Chapter 1 - Non-Newtonian fluid behaviour," in *Non-Newtonian Flow in the Process Industries*, R. P. Chhabra and J. F. Richardson, Eds. Oxford: Butterworth-Heinemann, 1-36.

[24] K. G. Skorpen, H. J. Roven, and O. J. J. o. M. P. T. Reiso, 2020. "A physical based empirical model for the accumulated strain in novel Metal Continuous Screw Extrusion (MCSE)," *Journal of Materials Processing Technology,* 282: 116670, DOI: https://doi.org/10.1016/j.jmatprotec.2020.116670.

[25] G. A. Campbell and M. A. Spalding, 2013. "The Melting Process," in *Troubleshooting and Analysis of Single-Screw Extrusion*, G. A. Campbell and M. A. Spalding, Eds.: Hanser, 189-245.

[26] Y. J. T. J. o. C. T. Marcus, 2017. "On the compressibility of liquid metals," *The Journal of Chemical Thermodynamics,* 109: 11-15. DOI: https://doi.org/10.1016/j.jct.2016.07.027.

[27] G. A. Campbell and M. A. Spalding, 2013, "Barrier and High-Performance Screws," in *Troubleshooting and Analysis of Single-Screw Extrusion*, 625-656. G. A. Campbell and M. A. Spalding, Eds.: Hanser,

[28] Z. J. I. m. r. Fan, 2002. "Semisolid metal processing," *International Materials Reviews,* 47(2): 49-85, DOI: https://doi.org/10.1179/095066001225001076.

[29] S. Nafisi, R. Ghomashchi, S. Nafisi, and R. J. S.-S. P. o. A. A. Ghomashchi, 2016, "Semi-Solid Metal (SSM) Technologies," in *Semi-Solid Processing of Aluminium Alloys*, S. Nafisi and R. Ghomashchi, Eds. Cham: Springer International Publishing. 9-48.

[30] W. Bleck, S. Dziallach, H. Meuser, W. Püttgen, and P. J. Uggowitzer, 2009. "Material Aspects of Steel Thixoforming," in *Thixoforming*, 43-104.

[31] S. Ji, K. Wang, and X. J. C. Dong, 2022. "An overview on the process development and the formation of non-dendritic microstructure in semi-solid processing of metallic materials," *Crystals,* 12(8): 1044. DOI: https://doi.org/10.3390/cryst12081044.

[32] S. Nafisi and R. J. C. m. q. Ghomashchi, 2005. "Semi-solid metal processing routes: an overview," *Canadian Metallurgical Quarterly.* 44(3): 289-304, DOI: https://doi.org/10.1179/cmq.2005.44.3.289.

[33] T. L. Bergman, 2011. *Fundamentals of Heat and Mass Transfer*. Wiley,

[34] S. Nafisi and R. Ghomashchi, 2016. "Methodology of SSM Characterization," in *Semi-Solid Processing of Aluminum Alloys*, S. Nafisi and R. Ghomashchi, Eds. Cham: Springer International Publishing, 81-149.

[35] B. R. Munson, A. P. Rothmayer, and T. H. Okiishi, 2012. *Fundamentals of Fluid Mechanics, 7th Edition*. Wiley,

[36] J.-h. Lin, H. Zhao, and J.-m. Huang, 2019. "Spatial interfacial heat transfer and surface characteristics during gravity casting of A356 alloy," *Transactions of Nonferrous Metals Society of China,* 29: 43-50, 01/01 DOI: https://doi.org/10.1016/S1003-6326(18)64913-1.

[37] P. Kiattisaksri *et al.*, 2010. "Assessment of the State of Precipitation in Aluminum Casting A356.2 Alloy Using Nondestructive Microstructure Electronic Property Measurements," *AIP Conference Proceedings,* 1211, 02/22. DOI: https://doi.org/10.1063/1.3362216.

[38] X. G. Hu *et al.*, 2017. "Blistering in semi-solid die casting of aluminium alloys and its avoidance," *Acta Materialia,* 124: 446-455, 2017/02/01/ DOI: https://doi.org/10.1016/j.actamat.2016.11.032.

[39] COMSOL, 2017. *CFD Module User's Guide*. COMSOL Inc.,

[40] C. Marschik, W. Roland, and T. A. J. P. Osswald, 2022. "Melt Conveying in Single-Screw Extruders: Modeling and Simulation," *Polymers.* 14(5): 875, DOI: https://doi.org/10.3390/polym14050875.

[41] I. Boumehdi, 2022."3d Printing Using Metallic Alloys In The Semisolid State," A Master Thesis, Department of Materials Science and Engineering, Politècnica de Catalunya University, Politècnica de Catalunya University,

[42] V. Abramov, O. Abramov, V. Bulgakov, and F. J. M. L. Sommer, 1998. "Solidification of aluminium alloys under ultrasonic irradiation using water-cooled resonator," *Materials Letters,* 37(1-2): 27-34, DOI: https://doi.org/10.1016/S0167-577X(98)00064-0.

[43] X. Jian, H. Xu, T. Meek, and Q. J. M. l. Han, 2005. "Effect of power ultrasound on solidification of aluminum A356 alloy," *Materials Letters,* 59(2-3): 190-193. DOI: https://doi.org/10.1016/j.matlet.2004.09.027.

[44] H.-c. Liao, G. Yuan, Q.-g. Wang, and D. J. T. o. N. M. S. o. C. Wilson, 2021. "Development of viscosity model for aluminum alloys using BP neural network," *Transactions of Nonferrous Metals Society of China,* 1(10): 2978-2985, DOI: https://doi.org/10.1016/S1003-6326(21)65707-2.

[45] B. Zhu, L. Li, X. Liu, L. Zhang, R. J. J. o. M. E. Xu, and Performance, 2015. "Effect of viscosity measurement method to simulate high pressure die casting of thin-wall AlSi10MnMg alloy castings," *Journal of Materials Engineering and Performance,* 4: 5032-5036, DOI: https://doi.org/10.1007/s11665-015-1783-8.